

Spin fluctuations in random magnetic-nonmagnetic two-dimensional antiferromagnets. III. An Ising system

R. A. Cowley,* R. J. Birgeneau,[†] and G. Shirane

Department of Physics, Brookhaven National Laboratory, Upton, New York 11973

H. J. Guggenheim

Bell Laboratories, Murray Hill, New Jersey 07974

H. Ikeda

*Department of Physics, Faculty of Science,
Ochanomizu University, Ohtsuka, Bunkyo-ku, Tokyo 112*

(Received 16 October 1979)

This paper reports a study using neutron scattering techniques of the spin fluctuations in the two-dimensional diluted Ising system, $\text{Rb}_2\text{Co}_c\text{Mg}_{1-c}\text{F}_4$. The explicit concentrations studied, $c = 0.55, 0.575, 0.585,$ and 0.595 are all close to the percolation concentration for nearest-neighbor interactions $c_p = 0.594$, so that these experiments span the percolation threshold. The experiments were performed at the Brookhaven high-flux beam reactor. A detailed study was made of the dynamics for $c = 0.575$. The results showed four dispersionless bands corresponding to spin deviations on Co ions surrounded by one, two, three, or four Co ions. Calculations of the spectra using the equation-of-motion method for computer simulations gave a good account of the results. The few minor discrepancies probably arise from the effects of those crystal-field levels of the Co ion which have energies above the ground-state doublet. The $c = 0.595$ crystal has a transition at 30 K to a state of two-dimensional order with negligible order in the third direction. The inverse correlation length in this system is zero to within the errors at 30 K. In the more dilute systems the inverse correlation length is found to be well described as an additive sum of a geometrical and a thermal part as observed previously in $\text{Rb}_2\text{Mn}_c\text{Mg}_{1-c}\text{F}_4$. The thermal part is given by $[\kappa_1(T)]^{1.32 \pm 0.05}$ where $\kappa_1(T)$ is the inverse correlation length of a one-dimensional chain of Co ions. This exponent is consistent with the percolation exponent $\nu_p = 1.35$ and the theoretically calculated crossover exponent, $\phi = 1$. The intensity of the scattering is more difficult to analyze in the absence of a knowledge of the form of the scaling function, but the behavior is consistent with the multicritical picture with $\phi = 1$.

I. INTRODUCTION

In the first two of this series of papers^{1,2} (hereafter referred to as I and II), we described the spin fluctuations in the random magnetic-nonmagnetic two-dimensional antiferromagnet, $\text{Rb}_2\text{Mn}_c\text{Mg}_{1-c}\text{F}_4$, in which system the Mn-Mn interactions are predominantly of Heisenberg character. In this paper we report on a very similar study of the analogous system, $\text{Rb}_2\text{Co}_c\text{Mg}_{1-c}\text{F}_4$, in which the magnetic interactions between the Co ions are of largely Ising character.³

In Paper II the theory behind the study of the percolation threshold in these materials was reviewed and discussed in detail. We only briefly repeat the description here. Basically the percolation point is believed to be a multicritical point which may be approached in two different ways. At $T = 0$ geometrically driven behavior is observed and may be described by exponents ν_p, β_p, γ_p , etc. while for $c = c_p$ thermally driven behavior is observed. The ap-

propriate temperature scale for the thermal behavior is set by the inverse correlation length $\kappa_1(T)$ of the one-dimensional chain with the magnetic interactions of the random system. In terms of this temperature scale the critical scattering for $c = c_p$ is governed by the exponents, ν_T and γ_T . In the multicritical picture the exponents ν_p and γ_p are related to ν_T and γ_T by the crossover exponent ϕ ; $\nu_p = \nu_T/\phi, \gamma_p = \gamma_T/\phi$. This study was commenced to test if this picture which successfully described our results for the Mn salts, II, was equally successful in explaining the properties of the Co system. In particular, since our initial study⁴ of the percolation threshold in the Mn systems, theoretical predictions^{5,6} of the crossover exponent ϕ have been made for a system with Ising interactions. These predictions are not in agreement with our results on the near Heisenberg system as discussed in II. Consequently it is of interest to study the Ising-like Co salt to test if these theoretical predictions are indeed correct.

The arrangement of the paper is that in Sec. II we describe the crystals used and the experimental arrangements for the neutron scattering experiments. A careful study of the spin dynamics was made for one of the specimens and these results are discussed in Sec. III. The quasielastic scattering associated with the percolation threshold was studied for four specimens, one of which was magnetically ordered at low temperatures. These results are discussed in Sec. IV. Finally the results are summarized in Sec. V.

II. EXPERIMENTAL DETAILS

A. Specimens

Single crystals of the mixed system $\text{Rb}_2\text{Co}_c\text{Mg}_{1-c}\text{F}_4$ were grown by techniques similar to those described for the $\text{Rb}_2\text{Mn}_c\text{Mg}_{1-c}\text{F}_4$ system.¹ Three crystals were grown with nominal concentrations c of, A , 0.55; B , 0.57; and C , 0.59. The resulting boules were typically about 5 cm long and shaped similarly to a dumbbell, and consisted of several large grains. Excellent single crystals with a volume of several centimeters cubed were obtained by cleaving these boules. A fourth smaller crystal, D , which was magnetically ordered at low temperatures, was grown by the methods described by Ikeda and Shirane⁷ with a nominal concentration of 0.59.

The crystal structure of Rb_2CoF_4 and of the mixed crystals is essentially similar to that of the analogous Mn salts which was described in Papers I and II. No evidence was found of any tendency for the Co and Mg ions to order chemically.

One of the most difficult aspects of experiments close to the percolation threshold is the determination of the exact concentration. All of these samples were analyzed by chemical methods by dissolving parts of the same boules and then using atomic-absorption spectroscopy to determine the concentrations. Measurements were made of the Co and Mg concentrations in two portions from each boule and

the averaged concentrations are shown in Table I.

Careful measurements were made of the lattice parameters in the a and c crystallographic directions. These results are listed in Table I and there is no significant difference between the different c lattice constants. A difference can be observed in the a lattice constants which, if the variation in lattice constant from Rb_2MgF_4 is linear in concentration $(1-c)$, suggests that the concentrations of crystals C and B differ by 0.035 ± 0.010 and C and A differ by 0.050 ± 0.010 .

In the case of $\text{Rb}_2\text{Mn}_c\text{Mg}_{1-c}\text{F}_4$ the comparison of the spin dynamics with computer simulations, Paper I, gave a very satisfactory determination of the concentration. Unfortunately this approach is less reliable in the Co system because the considerable absorption of the neutron beam by the Co nuclei combines with the irregular shape of the specimen to make the intensity distribution as a function of frequency less reliable than in the case of the Mn system.

We have shown in Fig. 2 of Paper II, the low-temperature inverse correlation lengths in $\text{Rb}_2\text{Mn}_c\text{Mg}_{1-c}\text{F}_4$ and $\text{Rb}_2\text{Co}_c\text{Mg}_{1-c}\text{F}_4$ as a function of concentration. For the Mn compound the concentrations were determined from the dynamical results as discussed above and from the lattice constant measurements. For $\text{Rb}_2\text{Co}_c\text{Mg}_{1-c}\text{F}_4$ we have taken for purposes of display in Fig. 2 of II the mean concentration as determined from the chemical analysis but with error limits that include both the concentrations of the starting material and the concentration differences inferred from the lattice-constant measurements. As we have emphasized in Paper II, all of the data are consistent with the simple law $\kappa_G(c) = 3(1 - c/0.594)^{1.35}$. If we take this law as given, then we may invert the process and use the measured low-temperature inverse correlation length to determine the concentration c . Indeed, if the Mn, Co, and Mg ions occupy the sites truly randomly during the crystal growth process, then for $c \leq c_p$ this would be by far the most accurate method of determining the concentration in this region. The internal con-

TABLE I. Characterization of the crystals.

Crystal	A	B	C	D
Nominal concentration	0.55	0.57	0.59	0.59
Chemical analysis	0.547 ± 0.030	0.578 ± 0.050	0.588 ± 0.030	0.612 ± 0.040
$\kappa(\Delta c, 0)a$	0.0893	0.0270	0.0120	0.045
Concentration from κa	0.550 ± 0.005	0.575 ± 0.005	0.583 ± 0.005	0.595 ± 0.020
c -axis lattice constant	13.732 ± 0.001	13.733 ± 0.001	13.734 ± 0.001	(13.670 Å, $c = 1$)
a -axis lattice constant	4.1060 ± 0.0003	4.1088 ± 0.0003	4.1102 ± 0.0003	(4.1440 Å, $c = 1$)

sistency of all of the results suggest that this is, in fact, the case. Accordingly, for samples *A*, *B*, and *C* we shall take as the concentrations 0.55, 0.575, and 0.585 which are the values suggested by κ_G . The concentration of sample *D* with $c > c_p$ was determined to be 0.595 ± 0.02 from the inverse correlation length as discussed in Sec. IV. Hereafter in this paper the different samples will be referred to by the above estimates of the concentration, that is, 0.55, 0.575, 0.585, and 0.595.

B. Neutron scattering measurements

The crystals were aligned with a magnetic [010] axis vertical in a variable-temperature cryostat and placed on a neutron spectrometer at the Brookhaven high-flux beam reactor. The measurements of the dynamics, in Sec. III, were performed with the spectrometer in the triple-axis configuration with pyrolytic graphite crystals as both monochromator and analyzer. The spectrometer was then operated with a fixed analyzer energy of 24 meV. The horizontal collimations throughout the spectrometer were $40'$ from reactor to counter, respectively, which gives a typical energy resolution of about 1.6 meV.

The quasielastic-scattering measurements were mostly performed as described in Paper II with a two-axis configuration with an incident neutron energy of 13.7 meV and 10 collimation throughout. Two pyrolytic graphite filters were used to remove the higher-order contaminants in the incident beam. The dimensions, full width at half maximum, of the resolution ellipse were determined for each crystal; they were typically 0.009 \AA^{-1} along the momentum transfer \vec{Q} , 0.002 \AA^{-1} perpendicular to \vec{Q} in the scattering plane and 0.1 \AA^{-1} vertically. Some experiments were performed with the crystal for which $c > c_p$ with relaxed horizontal collimation to improve the count rate for this smallest crystal and also with 5-meV incident neutrons and a cooled Be filter to try to separate the scattering from the ordered and disordered regions of this crystal below 30 K.

III. DYNAMICS

A. Experimental results

A study of the spin dynamics was made using the crystal with Co concentration $c = 0.575$. The results are illustrated in Fig. 1 for three different wave vectors in the Brillouin zone propagating along the magnetic [100] direction. The results show four peaks whose frequencies are almost independent of wave vector. This is similar to the results of Ikeda and Shirane⁷ on samples with a concentration of 0.7 and 0.89, although in the latter case the peak with the lowest frequency was not observed. The intensity of

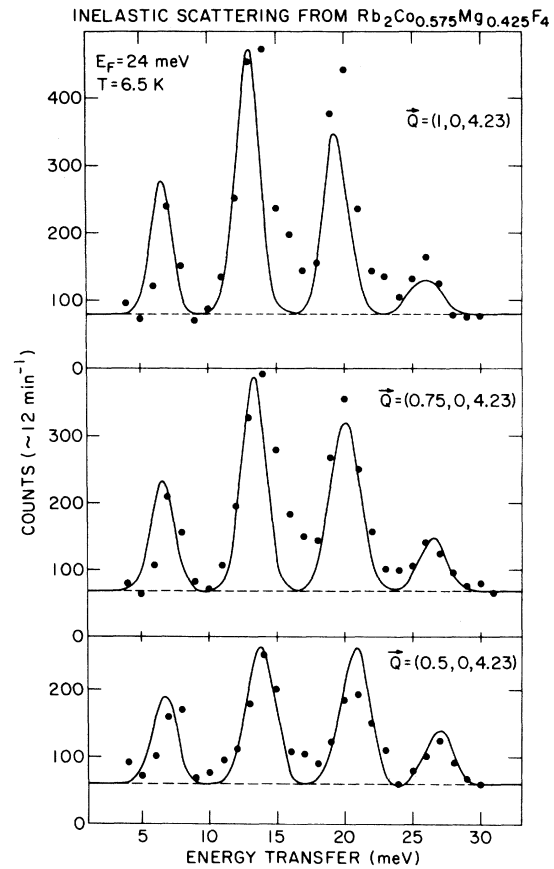


FIG. 1. The inelastic neutron scattering at 6.5 K from $\text{Rb}_2\text{Co}_{0.575}\text{Mg}_{0.425}\text{F}_4$ for three different wave-vector transfers. The experiments were performed with fixed outgoing neutron energy of 24 meV. The solid lines are the results of computer simulations convoluted with the experimental resolution. The dotted line is a frequency-independent background.

the scattering is approximately twice as large at the magnetic zone center as at the zone boundary.

The temperature dependence of the spectra was studied by warming to 60 K, and as shown in Fig. 2 there is only a slight broadening of the peaks in the scattered distributions. This temperature dependence is much less than that observed in the near Heisenberg system (Paper I), presumably because of the absence of low-energy excitations in the Ising-like system.

B. Theoretical models

The ground state of the Co ion in the tetragonal crystal field is a Kramers doublet, so that interactions within that doublet may be described by an effective Hamiltonian with spin $\frac{1}{2}$. The measurements³ of the spin excitations in Rb_2CoF_4 show that the excitations are well described by an effective Hamiltonian with

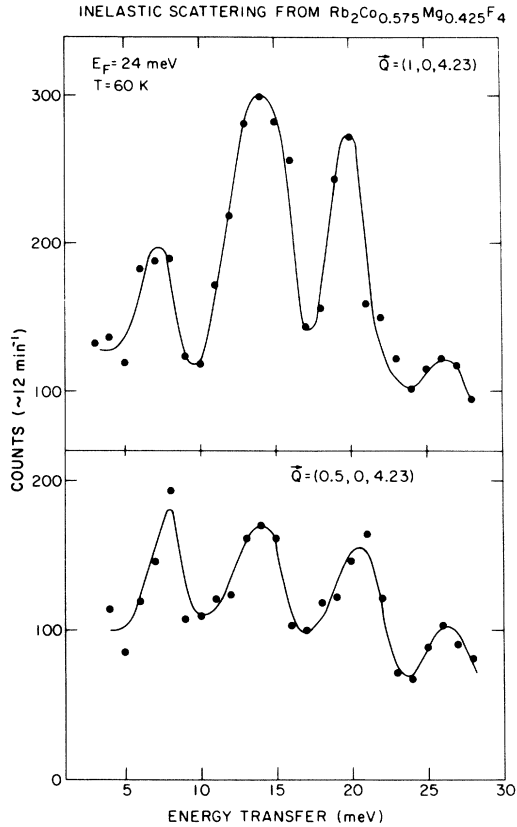


FIG. 2. The scattering at 60 K from the excitations in $\text{Rb}_2\text{Co}_{0.575}\text{Mg}_{0.425}\text{F}_4$. The experiments were performed with a fixed outgoing neutron energy of 24 meV, and the solid lines are guides to the eye.

anisotropic exchange between nearest neighbors;

$$H = \sum_{i,j} [IS_i^z S_j^z + J(S_i^x S_j^x + S_i^y S_j^y)] \quad (1)$$

with $I = 7.73 \pm 0.06$ meV and $J = 4.27 \pm 0.17$ meV. It is of interest to note that, for the two-dimensional (2D) Ising model, one would expect a phase-transition temperature $T_N = 1.135I/k_B = 101.8 \pm 0.8$ K; this is in precise agreement with the observed value of 102.06 K.

The simplest model of the excitations in a random system is the Ising model⁸ which in this case gives dispersionless frequencies of 0, I , $2I$, $3I$, and $4I$ corresponding to the frequencies of the excitations of Co ions surrounded by zero, one, two, three, or four Co nearest neighbors. This result is clearly an excellent qualitative description of the results shown in Fig. 1. The Ising model predicts that the scattered intensity is largely independent of wave-vector transfer.

A more careful examination of the experimental results indicates several inconsistencies with this simple model. First, the frequencies of the excitations show a small but significant dispersion with wave vector; the difference between the frequency of the

excitations at the zone boundary and at the zone center are, in order of decreasing frequency:

1.0 ± 0.4 , 0.9 ± 0.4 , 0.6 ± 0.4 , and 0.4 ± 0.4 meV.

Second, the frequencies at the zone boundary, 26.9 ± 0.4 , 20.7 ± 0.4 , 14.1 ± 0.4 , and 7.4 ± 0.4 meV, are not in the predicted ratios of 4, 3, 2, 1, but in the ratios of 3.64, 2.80, 1.91, 1. Third, the intensities are larger at the zone center than at the zone boundary by about a factor of 2; and, fourth, the highest frequency at the zone boundary is less than that in pure Rb_2CoF_4 , 30.8 meV even though as shown in Table I the a lattice parameter of the mixed system is slightly smaller than that of the pure system.

In order to study if these features arise from the transverse component of the exchange interaction, a computer simulation of the system was performed using the equation-of-motion method developed by Thorpe and Alben.⁹ This method was quite successful in describing our results for the dynamics of the Mn system as described in Paper I. When the calculations are performed with the exchange parameters taken to be those of pure Rb_2CoF_4 , the calculations give reasonable agreement with the wave-vector dependence of the frequency and intensity of the excitations. However, the predicted frequencies at the zone boundary are 29.7, 22.1, 14.3, and 6.8 meV which are clearly not in accord with our results.

A possible reason for this discrepancy lies in the inadequacy of the effective-spin- $\frac{1}{2}$ model for the Co ion. In a cubic crystal field the ground state¹⁰ is a Kramers doublet, $j = \frac{1}{2}$, separated in energy, by about 40 meV, from a quartet $j = \frac{3}{2}$. The tetragonal distortion of the crystal field splits this quartet into two Kramers doublets with $j_z = \pm \frac{1}{2}$ and $j_z = \pm \frac{3}{2}$. In the mixed crystal the Co ions are situated in the exchange field produced by the neighboring ions. The effect of this molecular field is to split the Kramers doublets and to mix the ground state with the $j_z = \pm \frac{1}{2}$ components of the excited state. As a result, the splitting in energy of the two lowest states is not linear in the molecular field but is given, for small molecular fields, by $H_{\text{MF}} - \alpha(H_{\text{MF}})^3$, where $H_{\text{MF}} = zI$ and z is the number of magnetic neighbors. When this result was used to calculate the Ising part of the energies in the computer simulations the frequencies of the excitations at the zone boundary were 26.9, 20.9, 13.9, and 6.7 meV when $I = 7.5$ meV and $\alpha = 0.00008$ meV⁻². These results are clearly in much better agreement with our measured results. The parameter α was estimated from the known properties of the Co ion in the lowest Hund's rule multiplet and the spin-orbit coupling of the free ion¹⁰ neglecting the tetragonal distortion as 0.00006 meV⁻². The results of these calculations are compared in detail with the experimental results in Fig. 1. The effective experimental resolution was taken as 1.6 meV and a single scale factor was adjusted to give

the best overall agreement. A flat background was subtracted from each distribution as shown in Fig. 1. In view of the unsymmetrical shape of the specimen and the high absorption of the neutron beam by the Co nuclei the agreement is very satisfactory.

The calculations were repeated with $\alpha=0$ and better resolution of 0.46 meV. The distributions then show considerable fine structure as illustrated in Fig. 3. We have not attempted to demonstrate the existence of this structure experimentally.

The only disquieting feature of our results is the decrease in the apparent exchange constant I . If we include the effect of the next crystal-field level the exchange constant I for pure Rb_2CoF_4 is increased to 8.47 suggesting that there is an 11% decrease in the exchange constant of the mixed crystal. Possibly this arises because of the increased importance of zero-point effects in the disordered system,¹¹ but we believe that this explanation is unlikely to account for such a large effect in a predominantly Ising-like material. A more likely explanation is again found in the construction of the effective-spin Hamiltonian for the Co ion. The effective interaction between the Co ions is possibly an exchange interaction J_T between the true spins, $S = \frac{3}{2}$. When this is projected into the ground state the molecular field of one ion on its neighbors is $J_T \langle S^z \rangle_G$, where $\langle S^z \rangle_G$ is the value of S^z in the ground state. Calculations¹² of $\langle S^z \rangle_G$ for KCoF_3 suggest that it increases by 40% as the molecular field increases from zero to its value in Rb_2CoF_4 . Consequently the effective exchange interaction I in the $S = \frac{1}{2}$ Hamiltonian increases as $\langle S^z \rangle_G$ or the molecular field increases. Since the average molecular field is about 60% in the mixed crystals of its value in the pure system, this effect accounts for the decrease in the effective exchange constant in the mixed crystals. Unfortunately a detailed description of these effects requires a precise knowledge of the crystal fields of the Co ion in these crystals and this requires considerably more study. In view, however,

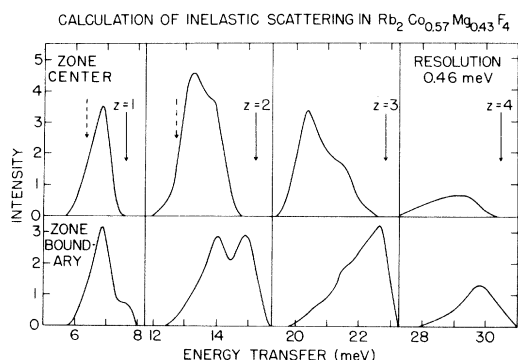


FIG. 3. The detailed shape of the neutron scattering in $\text{Rb}_2\text{Co}_{0.57}\text{Mg}_{0.43}\text{F}_4$ calculated using the computer simulation techniques of Thorpe and Alben (Ref. 9).

of the difficulties experienced in understanding the Co crystal-field levels in other Co compounds, such a study might well be rewarding.

In conclusion we believe that the spin dynamics in these systems are well understood and can be explained in detail using the computer simulation techniques of Alben and Thorpe. The slight discrepancies between theory and experiment probably result from the inadequacy of the $S = \frac{1}{2}$ effective-spin Hamiltonian for describing the excitations of the Co ion.

IV. PERCOLATION

A. Experimental results

The spin correlations close to the percolation point were measured with the spectrometer in a two-axis configuration to obtain the total scattering, $S(\vec{Q})$. In this configuration the scattering is wholly dominated by the scattering from the longitudinal fluctuations $\langle S^z(0)S^z(\vec{r}) \rangle$; from separate triple-axis measurements, this longitudinal scattering was found to be of quasielastic character with a width in energy which was determined by the spectrometer resolution.

A series of scans with wave vector $(\zeta, 0, 0.4)$ were performed to sample the scattering across the two-

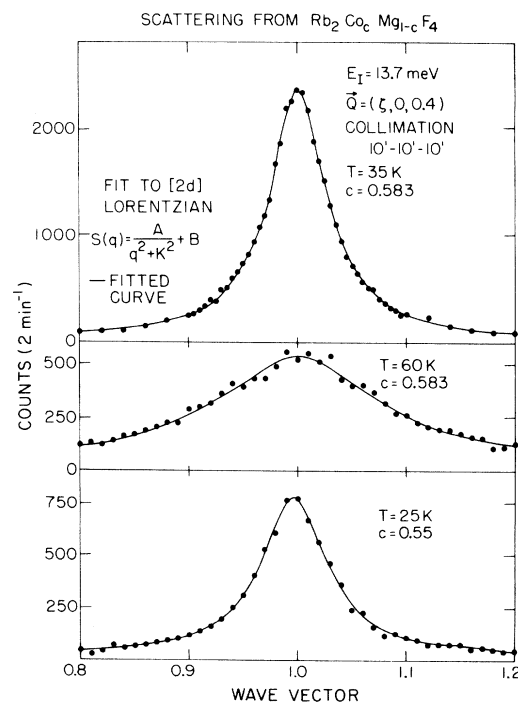


FIG. 4. The scattered intensity $S(\vec{Q})$ for $\vec{Q} = (\zeta, 0, 0.4)$ in $\text{Rb}_2\text{Co}_c\text{Mg}_{1-c}\text{F}_4$ at three different temperatures and concentrations. The solid lines are the best fits of two-dimensional Lorentzians to these results.

dimensional ridge of scattering $\zeta = 1$. Typical results of these scans are shown in Fig. 4. Scans were also performed with wave vectors $(1, 0, \eta)$ to sample the intensity along the top of the ridge as well as with wave vectors $(\zeta, 0, 0.4)$ with $\zeta \approx 3.0$. These scans confirmed the two-dimensional antiferromagnetic character of the scattering as reported in II for the Mn system.

The results were fitted in a least-squares sense to a two-dimensional

$$S(\bar{Q}) = |f(|\bar{Q}|)|^2 \left[1 - \frac{Q_z^2}{(\bar{Q})^2} \right] \frac{A}{q^2 + \kappa^2} \quad (2)$$

Lorentzian cross section, where $f(|\bar{Q}|)$ is the form factor of the Co ion¹³ and $\bar{q} = \bar{Q} - \bar{q}^*$ is the distance in wave-vector space of the momentum transfer \bar{Q} from the two-dimensional magnetic lattice line \bar{q}^* ; $q^2 = q_x^2 + q_y^2$. This form $S(\bar{Q})$ was convoluted with the measured resolution function of the spectrometer, added to a constant background and then fitted to the experimental results to obtain A and κ for each temperature and concentration by the method of least squares.

The goodness of fit as measured by χ^2 for the three specimens with $c < c_p$ in most cases was between 0.9 and 1.5, indicating, as shown in Fig. 4, that the two-dimensional Lorentzian form gives an

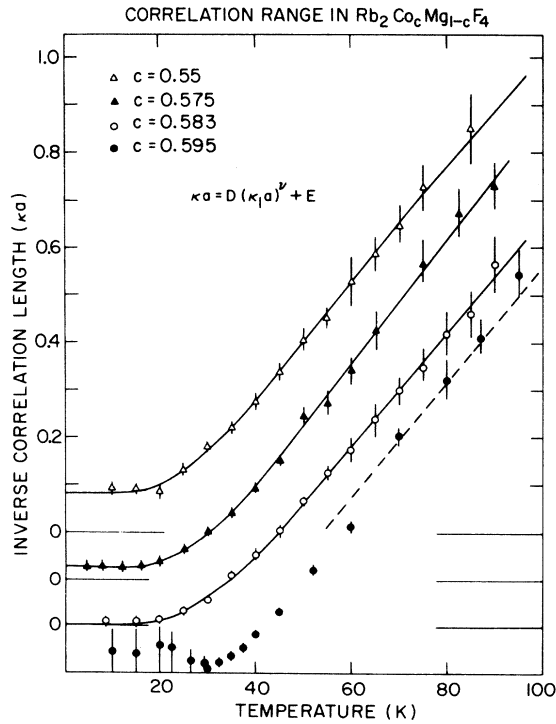


FIG. 5. The inverse correlation length in $\text{Rb}_2\text{Co}_c\text{Mg}_{1-c}\text{F}_4$ as a function of temperature. Note that the zeros of the scale are different for different c . For $c < c_p$ the solid lines are best fits to the form $\kappa a = D(\kappa_1 a)^{\eta T} + E$.

excellent description of these results. Similar success was achieved in the near-Heisenberg system (Paper II). The temperature dependence of the inverse correlation length κ and of the amplitude A are shown in Figs. 5 and 6, respectively. Since the specimens with different c have different volumes, the amplitudes A have been arbitrarily scaled to be approximately constant at high temperatures. For the samples with $c < 0.59$, κ decreases with decreasing temperature and becomes almost constant for $T < 20$ K. The minimum value of κ is smaller the larger the concentration, as shown in Table I. The amplitude has a similar variation although the decrease with decreasing temperature is less marked than for the correlation length.

Similar measurements were performed for the sample with $c = 0.595$. A good fit to the results was obtained for $T > 30$ K when they were fitted to Eq. (2). At lower temperatures, however, the fit was very poor $\chi^2 \approx 100$. When the points in the scan within the resolution function width of $\zeta = 1.00$ were omitted, good fits could be obtained to the data outside of this region of wave vector as illustrated in Fig. 7. We believe that the additional intensity for $\zeta \sim 1.0$ arises from a two-dimensional Bragg-reflection line due to

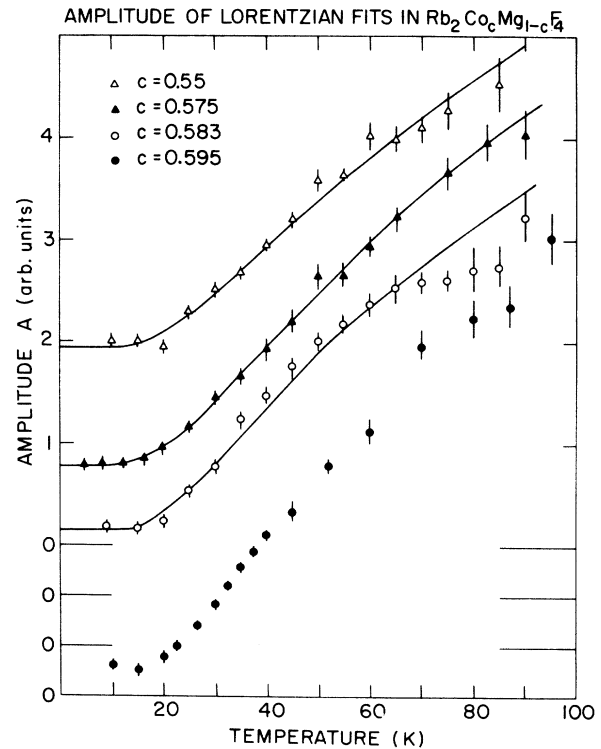


FIG. 6. The amplitude of the scattering A in $\text{Rb}_2\text{Co}_c\text{Mg}_{1-c}\text{F}_4$. Note that the zeros of the scale are different for different c and that the normalization from one c to another was adjusted to bring A at high temperatures nearly constant. The solid lines for $c < c_p$ are best fits to $A = D_1(\kappa_1 a)^{\eta T} + E_1$.

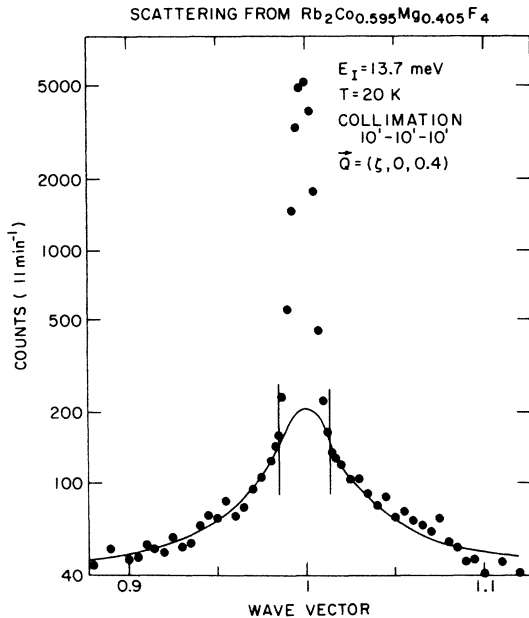


FIG. 7. Scattering from $\text{Rb}_2\text{Co}_c\text{Mg}_{1-c}\text{F}_4$ with $c = 0.595$ and $T = 20$ K. The solid line is a fit with a two-dimensional Lorentzian to the points outside the region indicated by the vertical lines. This region is a resolution width around $\zeta = 1.00$ and the additional scattering in this region demonstrates the existence of two-dimensional long-range order.

the development of two-dimensional long-range order below 30 K. The temperature dependence of this Bragg scattering is illustrated in Fig. 8. Since the concentration dependence of T_c in this Ising system is predicted¹⁴ to vary as $|\ln(c - c_p)|^{-1}$, only very small fluctuations in concentration should give rise to

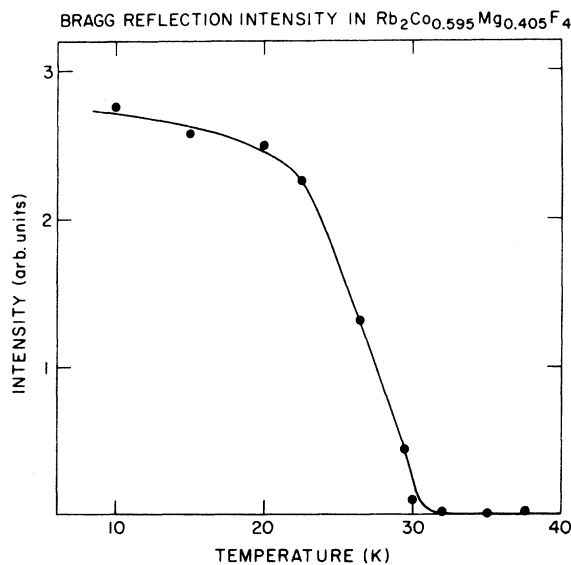


FIG. 8. The intensity of the two-dimensional Bragg scattering in $\text{Rb}_2\text{Co}_c\text{Mg}_{1-c}\text{F}_4$ with $c = 0.595$.

very large changes in T_c . Consequently it is very unlikely, albeit unfortunate, that a reliable estimate of the exponent β can be obtained from Fig. 8.

The result of a scan along the two-dimensional Bragg line $(1,0,\eta)$ is shown in Fig. 9. The wave-vector dependence expected from the form factor and geometrical factors, Eq. (1), is shown by the solid line. Clearly the ordering is, within the errors, of ideal two-dimensional character with negligible ordering in the third direction. This result differs from that in the Mn system where for c slightly larger than c_p the system develops two-dimensional order but with some correlation, ~ 40 Å, perpendicular to the planes. This ordering perpendicular to the magnetic sheets is absent in the Co salts, presumably because the magnetic dipolar interactions between the planes are somewhat weaker in the Co system than in the Mn system and, more importantly, because the Ising system more readily becomes frozen at low temperatures than the near-Heisenberg system which has significant low-energy excitations.

It is also interesting to compare these results with those of Ikeda *et al.*¹⁵ on the same system but with $c = 0.89, 0.85,$ and 0.7 . Their results indicated that the correlation between the magnetic sheets decreased with decreasing c and was also dependent upon the rate of cooling through T_N . Our measurements show that this correlation is entirely suppressed for $c = 0.595$.

The analysis of the diffuse scattering in this specimen yielded the inverse correlation lengths and amplitudes as illustrated in Figs. 5 and 6. The inverse correlation length equals 0 \AA^{-1} within the experimental error at 30 K where the long-range order develops and then appears to increase with a further decrease in temperature. The amplitude A is monotonically decreasing until $T < 20$ K. Around 30 K A decreases much more rapidly than in the case of the specimens for $c < c_p$.

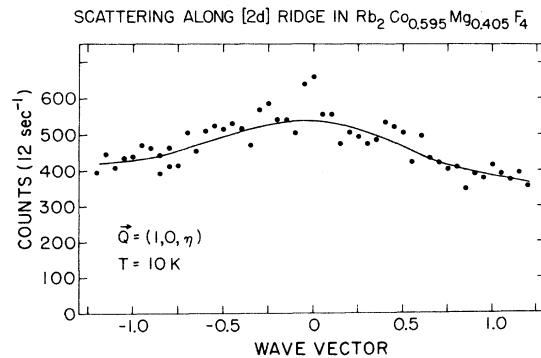


FIG. 9. Scattering $S(\vec{Q})$ for $\vec{Q} = (1, 0, \eta)$ in $\text{Rb}_2\text{Co}_c\text{Mg}_{1-c}\text{F}_4$ for $c = 0.595$ and $T = 10$ K. The solid line gives the wave-vector dependence due to the form factor and geometrical factors if the ordering is two dimensional in character.

B. Analysis of the experimental results

For the reasons described in Paper II, the natural temperature scale $\mu(T)$ for describing percolation phenomena is the inverse correlation length $\kappa_1(T)$ of the one-dimensional chain with the same magnetic interactions as occur in the system. κ_1 may be calculated exactly for an Ising linear chain as

$$\mu(T) = \kappa_1 a = [(1-u)^2/u]^{1/2}, \quad (3)$$

where $u = \tanh(1/kT)$. In our calculations of κ_1 we have used $I = 7.4$ meV so that the frequency of the excitations with lowest frequency, in Sec. III, was given correctly. Initially we examined the form suggested for the scattering by Eqs. (19) and (20) of II, in particular that κ is the sum of a geometrical and a thermal part

$$\kappa = \kappa(\Delta c, 0) + \kappa(0, \mu). \quad (4)$$

The results for κ shown in Fig. 5 suggest that this is indeed a reasonable approximation for $c < c_p$ because the curves for κ for each concentration are displaced from one another by an amount which is at least approximately independent of temperature. In order to examine this hypothesis further we performed fits of the data to Eq. (4) with

$$\kappa(0, \mu)a = D \mu^{\nu_T} = D (\kappa_1 a)^{\nu_T}.$$

The results are listed in Table II, and illustrated in Fig. 5. Clearly the fit gives a good description of the experimental results. Some fits were also performed with ν_T held fixed¹⁶ at 1.33. These fits are illustrated in Fig. 10 where κa is shown plotted against $\kappa_1 a$.

The results of this analysis for several concentrations suggest that $\nu_T = 1.32 \pm 0.04$ and that $D = 0.96 \pm 0.06$.

The amplitude of the scattering A was analyzed in two different ways. First, as suggested from the arguments given in Paper II, Eq. (20), fits were performed assuming that

$$A = D_2 (\kappa a)^{\eta_T}, \quad (5)$$

or equivalently $S(q) = A \kappa^\eta / (\kappa^2 + q^2)$ with κ given by Eq. (4). This expression gave a good description of our results as shown in Fig. 11 and the parameters

TABLE II. Least-squares fits to κa .

Concentration	χ^2	D	$\kappa(\Delta c, 0)a$	ν_T
0.55	1.32	0.96 ± 0.01	0.085 ± 0.004	1.16 ± 0.05
0.575	0.68	1.00 ± 0.02	0.026 ± 0.004	1.31 ± 0.03
0.583	0.59	0.93 ± 0.02	0.004 ± 0.004	1.33 ± 0.06
0.55	2.31	1.09 ± 0.04	0.092 ± 0.004	1.33
0.575	0.73	1.03 ± 0.02	0.032 ± 0.002	1.33
0.583	0.40	0.92 ± 0.02	0.007 ± 0.004	1.33

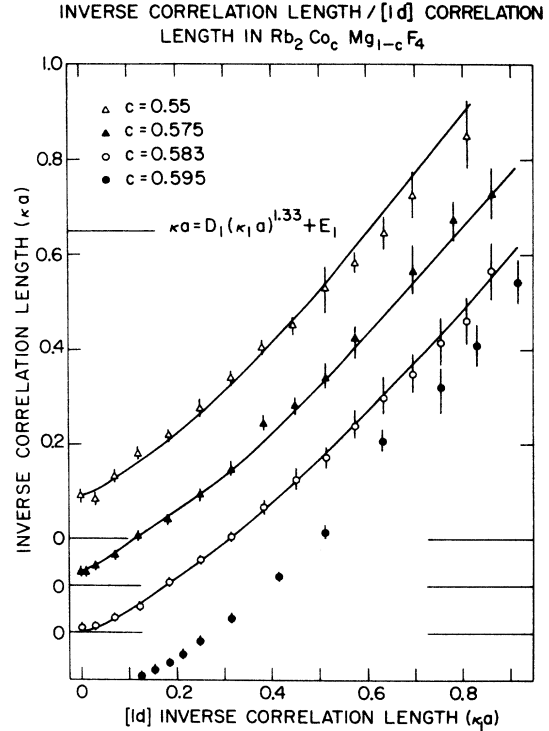


FIG. 10. The inverse correlation length κa for $\text{Rb}_2\text{Co}_c\text{Mg}_{1-c}\text{F}_4$ plotted against $\kappa_1 a$, the appropriate one-dimensional correlation length. Note the different zeros for the different concentrations. The solid lines are fits to $\kappa a = D_1(\kappa_1 a)^{1.33} + E_1$.

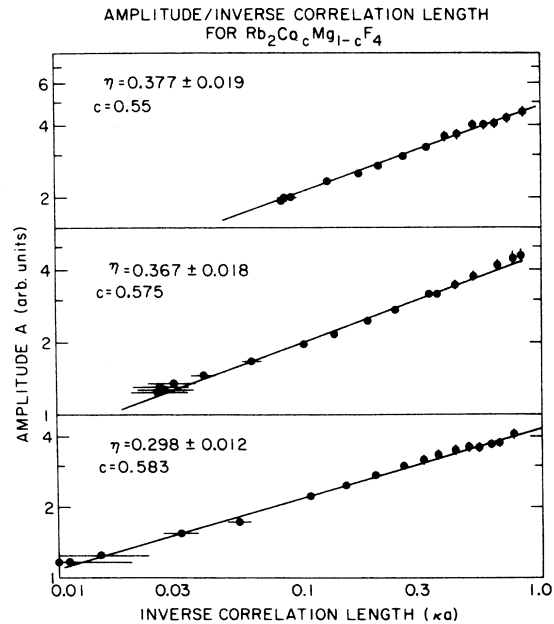


FIG. 11. The amplitude A plotted against the correlation length κa for three concentrations of $\text{Rb}_2\text{Co}_c\text{Mg}_{1-c}\text{F}_4$.

TABLE III. Least-squares fits to A .

Concentration	χ^2	Eq. (5)	
		η_T	$\gamma_T = \nu_T(2 - \eta_T)$
0.55	0.23	0.38 ± 0.02	1.88 ± 0.07
0.575	0.79	0.38 ± 0.02	2.12 ± 0.06
0.583	1.15	0.30 ± 0.01	2.26 ± 0.06
Concentration	χ^2	Eq. (6)	
		λ_T	F
0.55	0.23	0.89 ± 0.07	0.58 ± 0.05
0.575	0.79	0.87 ± 0.02	0.33 ± 0.02
0.583	1.15	0.96 ± 0.08	0.23 ± 0.02

η_T which are listed in Table III show that the fitted η_T is not too dependent on concentration. As discussed in Paper II, the susceptibility exponent γ_T may be obtained using the scaling relation $\gamma_T = \nu_T(2 - \eta_T)$; the results so obtained are listed in Table III.

In view of the uncertainty in the functional form of the scattering, we also performed fits to A with the expression

$$A = E[(\kappa_1 a)^{\lambda_T} + F] \quad (6)$$

This function also gave a very reasonable account of the results as shown in Fig. 6 and the significant parameters λ_T and F are listed in Table III.

We have also fitted the reciprocal of the intensity

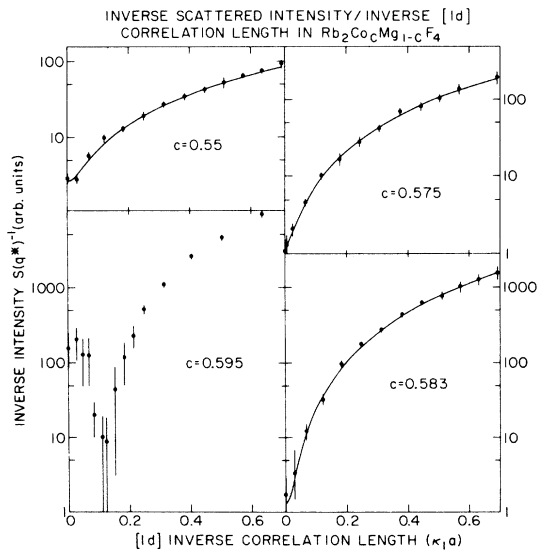


FIG. 12. The reciprocal of the intensity $S(q^*)$ for four concentrations as a function of $\kappa_1(T)$ in $\text{Rb}_2\text{Co}_c\text{Mg}_{1-c}\text{F}_4$. The solid lines are fits to the form $S(q^*) = G[(\kappa_1 a)^{\gamma_T} + H]$.

at the magnetic zone center to the form

$$S(q^*) = G[(\kappa_1 a)^{\gamma_T} + H]^{-1} \quad (7)$$

The results are shown in Fig. 12 for $c < c_p$, and this form also accounts well for our experimental results. The parameters γ_T and H are listed in Table IV.

The diffuse scattering for the sample with $c = 0.595$ is more difficult to analyze. At high temperatures, $T \geq 70$ K, the inverse correlation length κ is possibly larger than for the $c = 0.583$ crystal as shown in Fig. 5. The dotted line shows the fit to the $c = 0.583$ data for $T > 60$ K plotted against the $c = 0.595$ results. The results shown in Fig. 5 show for $c < c_p$ that κ decreases with increasing c at high temperatures. If we assume, as seems very reasonable, that this behavior continues for $c > c_p$, the high-temperature results show that the $c = 0.595$ specimen has c very close to c_p . If we further assume that $\kappa_G(c) = 3|1 - c_p/0.594|^{1.35}$ we obtain for this specimen $c = 0.595 \pm 0.02$ as listed in Table I.

As the phase transition is approached, the system presumably undergoes a crossover from percolation-dominated behavior to Ising two-dimensional random behavior.¹⁷ If the measurements of the correlation length (κa) between 35 and 60 K are used to determine an exponent ν , $\kappa a \approx (T - T_c)^\nu$, then we find $T_c = 31$ K and $\nu = 1.06 \pm 0.15$. A similar analysis of the intensity $S(q^*)$ leads to an exponent for the susceptibility γ of 1.8 ± 0.3 . In view of the fact that the transition is probably smeared and that we do not

TABLE IV. Least-squares fits to $S(q^*)^{-1}$ using Eq. (7).

Concentration	χ^2	γ_T	H
0.55	0.54	1.53 ± 0.07	0.020 ± 0.002
0.575	0.30	1.79 ± 0.04	0.0034 ± 0.0015
0.583	0.56	2.17 ± 0.06	0.0004 ± 0.0004

know the crossover temperature, the agreement with the exponents of the two-dimensional Ising model¹⁸ $\nu = 1$, $\gamma = 1.75$ is fortuitously good. It is clearly impossible to determine the exponents below T_c from these experiments. Similar results in agreement with the two-dimensional Ising model and a smeared transition were found for $c = 0.82, 0.89, 0.95, 0.97$, and 0.98 by Ikeda *et al.*¹⁹

V. DISCUSSION OF THE RESULTS

A. Percolation threshold

The multicritical-point picture of percolation was described in detail in Paper II, and in this section we review the extent to which the behavior described in the preceding section is compatible with this picture. In the Ising system the crossover exponent ϕ connecting the geometrical and thermal behavior is believed to be unity^{5,6} so that the exponents describing the geometrical and thermal behavior are equal; that is $\gamma_p = \gamma_T$, $\nu_p = \nu_T$, etc. In the analysis of our results we have assumed particularly simple forms for the scaling functions such as Eqs. (3)–(6).

The results for the correlation length strongly support the validity of Eq. (4), namely, that the inverse correlation length is the sum of a geometrical and thermal part. Furthermore, the thermal part is given by $D(\kappa_1 a)^{\nu_T}$ with $D = 0.96 \pm 0.06$ and $\nu_T = 1.32 \pm 0.04$. This result is in excellent agreement with the best¹⁷ estimate of $\nu_p = 1.356$ and a crossover exponent of unity. The constant D has not been obtained theoretically but it is interesting that within error it is identical for Heisenberg-like (Paper II) and Ising-like systems and with the exact result in one dimension as discussed in Paper II.

The analysis of the amplitude is more complex; in part this is because of the difficulty of reliably scaling the intensity from one crystal to another. When it is assumed that $A \sim (\kappa a)^{\eta_T}$, Eq. (5), we obtain, in Table III, results which suggest that η_T is possibly concentration dependent. A reasonable estimate for η_T from our results for different concentrations is $\eta_T = 0.32 \pm 0.08$ which is in excellent agreement with η_T for the Mn system 0.30 ± 0.15 , and is in fair agreement with the best estimate¹⁶ of $\eta_p = 0.204$. The situation is, however, less satisfactory if we consider the fits done to Eq. (6). In this case λ_T is roughly independent of concentration and $\lambda_T = 0.91 \pm 0.05$. Since $\lambda_p = \eta_p \nu_p$, the best theoretical estimate of λ_p is 0.28 which is very different from our results. This difference arises because Eq. (6) introduces independent geometrical and thermal contributions to A , while in Eq. (5) the ratio of these two contributions is assumed to be the same as in the inverse correlation length. The difference between the exponents derived from these two forms illustrates the difficulty of reliably extracting the exponents near

a multicritical point without a detailed knowledge of the scaling functions.

Finally, the exponent γ_T was obtained in two different fashions; the two sets of results are listed in Tables III and IV. For both assumed functional forms for $S(q^*)$, the fitted $\gamma_T(c)$ increases monotonically with c as c approaches c_p ; clearly this shows that neither Eq. (5) nor Eq. (7) is adequate for c away from c_p and once more this highlights the need for a more complete theory of magnetism near the percolation multicritical point. We should emphasize that at $c = c_p$ both Eq. (5) and Eq. (7) reduce to $S(q^*) \sim (K_1 a)^{\gamma_T}$ which is almost certainly correct to leading order. This suggests on a heuristic basis that one should extrapolate the values deduced from $\gamma_T(c)$ to $c = c_p$. From a simple linear extrapolation we deduce $\gamma_T(c_p) = 2.4 \pm 0.1$. This is in agreement with the $\phi = 1$ theoretical value of $\gamma_T = \gamma_p = 2.43 \pm 0.03$.

B. Summary

The excitations in the mixed two-dimensional near-Ising model $\text{Rb}_2\text{Co}_c\text{Mg}_{1-c}\text{F}_4$ with $c = 0.575$ were measured at 6.5 K. The results show four almost dispersionless branches which are qualitatively in agreement with the predictions of a simple Ising model. Computer simulations have been performed to include the transverse interactions but some small discrepancies still remained between experiment and theory. We believe these arise from inadequacies in the effective $S = \frac{1}{2}$ model for the lowest levels of the Co ion due to the mixing with higher crystal-field levels. More work is needed to determine the crystal fields in detail before a quantitative theory of these effects is possible.

Detailed quasielastic measurements were made of four specimens with c close to the percolation limit c_p . These measurements could all be described by a two-dimensional Lorentzian except for $c > c_p$ at low temperatures where, in addition, the measurements showed a Bragg line from the two-dimensional long-range order. The correlation length diverged at the onset of long-range order and the divergence in both the intensity and correlation length were consistent with the behavior of the two-dimensional Ising model.

The behavior of the scattering close to c_p provides strong support for the multicritical picture of the percolation point. The inverse correlation length can be expressed as the sum of a geometrical and thermal part, and the thermal part behaves as the inverse correlation length of a linear chain of Co ions to the power 1.32 ± 0.04 . This is in excellent accord with a crossover exponent $\phi = 1$ as obtained for Ising systems theoretically. The results for the amplitude or intensity are also consistent with this picture. This statement is, however, weaker than that for the inverse correlation length because there are a variety of

descriptions of our results, and in the absence of a knowledge of the appropriate multicritical point scaling functions it is difficult to choose between these descriptions. Nevertheless, with an optimistic extrapolation to $c = c_p$, we deduce $\gamma_T = 2.4 \pm 0.1$ in agreement with the $\phi = 1$ theory. We hope that these results will stimulate further work on this aspect of the problem.

ACKNOWLEDGMENTS

The work at Brookhaven was supported by the Division of Basic Energy Sciences, Department of Energy, under Contract No. EY-76-C-02-0016, at Edinburgh by the Science Research Council, and at MIT by the National Science Foundation Materials Research Laboratory, Grant No. DMR-76-80895.

*Permanent address: Dept. of Physics, University of Edinburgh, Scotland.

†Permanent address: Dept. of Physics and Center for Materials Science and Engineering, Massachusetts Institute for Technology, Cambridge, Mass. 02139.

¹R. A. Cowley, G. Shirane, R. J. Birgeneau, and H. J. Guggenheim, *Phys. Rev. B* **15**, 4292 (1977).

²R. J. Birgeneau, R. A. Cowley, G. Shirane, J. A. Tarvin, and H. J. Guggenheim, *Phys. Rev. B* **21**, 317 (1980).

³H. Ikeda and M. T. Hutchings, *J. Phys. C* **11**, L529 (1978).

⁴R. J. Birgeneau, R. A. Cowley, G. Shirane, and H. J. Guggenheim, *Phys. Rev. Lett.* **37**, 940 (1976).

⁵M. J. Stephen and G. S. Grest, *Phys. Rev. Lett.* **38**, 567 (1977).

⁶D. J. Wallace and A. P. Young, *Phys. Rev. B* **17**, 2384 (1978).

⁷H. Ikeda and G. Shirane, *J. Phys. Soc. Jpn.* **46**, 30 (1979).

⁸For a review see R. A. Cowley, in *Proceedings of the Twenty-first International Conference on Magnetism and Magnetic Materials, Philadelphia, Pennsylvania, 1975*, edited by J. J. Becker, G. H. Lander, and J. J. Rhyne, AIP Conf. Proc. No. 29 (AIP, New York, 1976), p. 243.

⁹M. F. Thorpe and R. Alben, *J. Phys. C* **8**, L275 (1975); **9**, 2555 (1976).

¹⁰J. M. H. Thornley, C. G. Windsor, and J. Owen, *Proc. R. Soc. London Ser. A* **284**, 252 (1965).

¹¹J. W. Halley and W. K. Holcomb, *J. Appl. Phys.* **49**, 2153 (1978).

¹²W. J. L. Buyers, T. M. Holden, E. C. Svensson, R. A. Cowley, and M. T. Hutchings, *J. Phys. C* **4**, 2139 (1971).

¹³R. E. Watson and A. J. Freeman, *Acta Crystallogr.* **14**, 27 (1961).

¹⁴D. Stauffer, *Z. Phys. B* **22**, 161 (1975); T. C. Lubensky, *Phys. Rev. B* **15**, 311 (1976).

¹⁵H. I. Ikeda, M. T. Hutchings, and M. Suzuki, *J. Phys. C* **11**, L359 (1978).

¹⁶When these fits were performed 1.33 was believed to be the best estimate of $\nu_T = \nu_p$; H. E. Stanley, *J. Phys. A* **10**, L211 (1977). The best estimate is currently 1.356; P. J. Reynolds, H. E. Stanley, and W. Klein, *J. Phys. A* **11**, L199 (1978). The difference would not, however, make an appreciable difference to the fits shown in Fig. 10.

¹⁷The critical behavior of a site-random two-dimensional Ising model is not completely certain, but, since the specific-heat exponent is zero, it is believed to be that of the pure-Ising model, together with possible logarithmic corrections. Experiments supporting this and relevant theoretical references are given by R. J. Birgeneau, J. Als-Nielsen, and G. Shirane, *Phys. Rev. B* **16**, 280 (1977).

¹⁸H. E. Stanley, *Introduction to Phase Transitions and Critical Phenomena* (Oxford Univ. Press, New York, 1971).

¹⁹H. Ikeda, M. Suzuki, and M. T. Hutchings, *J. Phys. Soc. Jpn.* **46**, 1153 (1979).